JOC The Journal of Organic Chemistry

Article

pubs.acs.org/joc

5-Carboxamido-5-formamido-2-iminohydantoin, in Addition to 8-oxo-7,8-Dihydroguanine, Is the Major Product of the Iron-Fenton or X-ray Radiation-Induced Oxidation of Guanine under Aerobic Reducing Conditions in Nucleoside and DNA Contexts

Omar R. Alshykhly, Aaron M. Fleming, and Cynthia J. Burrows*

Department of Chemistry, University of Utah, 315 S 1400 East, Salt Lake City, Utah 84112-0850, United States

Supporting Information

ABSTRACT: Exogenously and endogenously produced reactive oxygen species attack the base and sugar moieties of DNA showing a preference for reaction at 2′-deoxyguanosine (**dG**) sites. In the present work, **dG** was oxidized by HO$^{\bullet}$ via the Fe(II)-Fenton reaction or by X-ray radiolysis of water. The oxidized lesions observed include the 2′-deoxynucleosides of 8-oxo-7,8-dihydroguanine (**dOG**), spiroiminodihydantoin (**dSp**), 5-guanidinohydantoin (**dGh**), oxazolone (**dZ**), 5-carboxamido-5-formamido-2-iminohydantoin (**d2Ih**), 5′,8-cyclo-2′-deoxyguanosine (**cyclo-dG**), and the free base guanine (**Gua**). Reactions conducted with ascorbate or *N*-acetylcysteine as a reductant under aerobic conditions identified **d2Ih** as the major lesion formed. Studies were conducted to identify the role of O_2 and the reductant in product formation. From these studies, mechanisms are proposed to support **d2Ih** as a major oxidation product detected under aerobic conditions in the presence of the reductant. These nucleoside observations were then validated in oxidations of oligodeoxynucleotide and λ-DNA contexts that demonstrated high yields of **d2Ih** in tandem with **dOG**, **dSp**, and **dGh**. These results identify **dG** oxidation to **d2Ih** to occur in high yields leading to a hypothesis that **d2Ih** could be found from in cells stressed with HO$^{\bullet}$. Further, the distorted ring structure of **d2Ih** likely causes this lesion to be highly mutagenic.

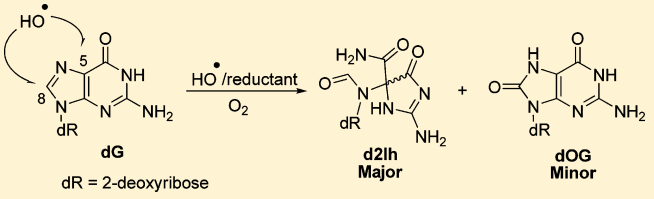

INTRODUCTION

Cellular redox status is a dynamic state that balances reducing and oxidizing species, and if the balance is thrown off in the cell, dysfunction arises.[1] The hydroxyl radical (HO$^{\bullet}$) is a powerful oxidizing species found in the cell and causes redox imbalance due to its particularly high redox potential (2.31 V vs NHE, pH 7; HO$^{\bullet}$(+H^{+})/H_2O).[2] The Fenton reaction can generate HO$^{\bullet}$ when a redox-active metal effects cleavage of H_2O_2, a metabolic product that can easily diffuse within and between cells.[3] Hydrogen peroxide is weakly reactive, but Fe(II) species have the capability to generate HO$^{\bullet}$ plus Fe(III) via the Fenton reaction (Reaction 1). Furthermore, reducing agents in the cell such as ascorbate (Asc) allow this reaction to be catalytic in iron by reducing Fe(III) back to Fe(II) (Reaction 2).[4,5] The unfortunate events that occurred at Fukushima, Japan in 2011 remind us of the dangers of radiation. The high-energy photons released upon radioactive decay are capable of yielding HO$^{\bullet}$ via radiolysis of water (Reactions 3 and 4). The iron-Fenton reaction and X-ray radiolysis of water represent two methods for generating hydroxyl radicals that can oxidize biomolecules[6,7] such as DNA.[4,5,8] DNA damage plays a significant role in aging, and the development of diseases such as cancer.[8]

$$H_2O_2 + Fe(II) \rightarrow Fe(III) + HO^{\bullet} + HO^{-} \quad (1)$$

$$2Fe(III) + Asc \rightarrow 2Fe(II) + \text{dehydroascorbate} \quad (2)$$

$$H_2O + \text{X-ray} \rightarrow e^{-}_{aq} + H_2O^{+} \quad (3)$$

$$H_2O^{+} \rightarrow H^{+} + HO^{\bullet} \quad (4)$$

DNA is vulnerable to oxidative insults from HO$^{\bullet}$, and the damage is particularly deleterious because it can cause mutations that are heritable to daughter cells. Notable progress has been made in the discovery of DNA oxidation pathways resulting from radical oxygen species, such as HO$^{\bullet}$, during the past three decades.[4,9−12] In DNA, the most susceptible site is 2′-deoxyguanosine (**dG**) because the guanine heterocycle has the lowest redox potential (1.29 V vs NHE, pH 7; **dG**$^{\bullet}$(−H^{+})/**dG**) among the four DNA bases.[13] The nucleoside **dG** is a prime target for direct oxidation or electron transfer-mediated oxidation that can result from HO$^{\bullet}$.[10,13,14] Oxidative damage to **dG** yields products that result from the initial product-forming reaction occurring at one of three sites that include the C5 or C8 positions of the heterocyclic ring, or the 2-deoxyribose unit (Figure 1). These products are identified by their characteristic mass changes from the parent nucleoside **dG** (**M**).

Sugar oxidation is a commonly observed reaction pathway of **dG** damage resulting from HO$^{\bullet}$.[12] Products observed along this pathway include 5′,8-cyclo-2′-deoxyguanosine (**cyclo-dG**)

Received: March 27, 2015
Published: June 19, 2015

DOI: 10.1021/acs.joc.5b00689
J. Org. Chem. 2015, 80, 6996−7007

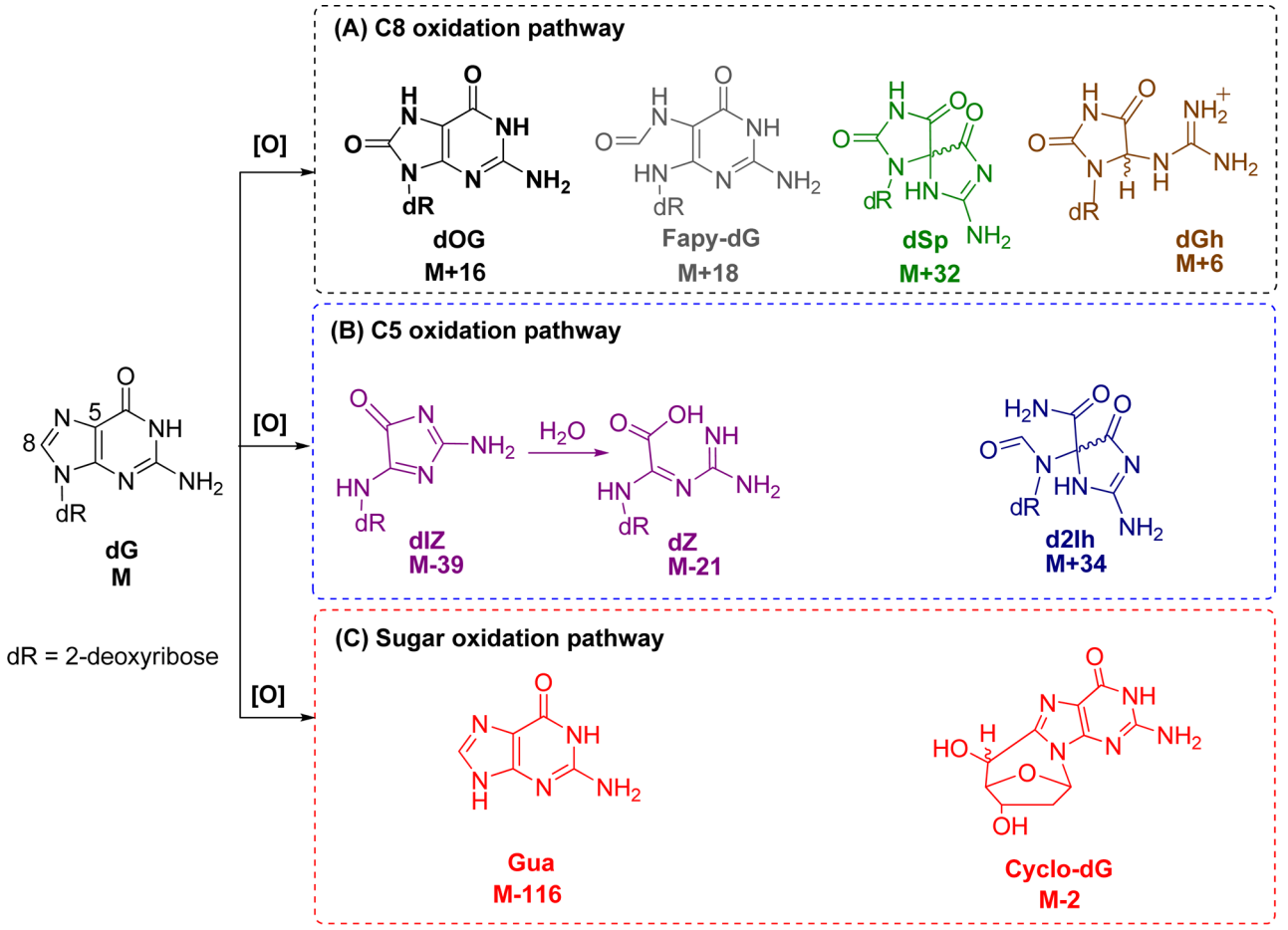

Figure 1. Structures of **dG** and its oxidation products. Box A: products observed from initial HO• attack at C8. Box B: products observed from initial HO• attack at C5. Box C: guanine-derived products observed when oxidation occurs on 2-deoxyribose.

diastereomers derived from H• atom abstraction at C5′, and release of the free base guanine (**Gua**) after hydroxylation of C1′. Direct base release in DNA leads to strand breaks due to the lability of the abasic site so formed.[15−17] The yields of these products are highly dependent on the reaction conditions.[12] Base oxidation of **dG** leads to two lesions resulting from reaction at C8 that include 8-oxo-7,8-dihydro-2′-deoxyguanosine (**dOG**), observed in high yield under aerobic oxidizing conditions, or the ring-opened product 2,6-diamino-4-hydroxy-5-formamidopyrimidine-2′-deoxyribonucleoside (**Fapy-dG**) observed under anaerobic reducing conditions.[18−20] Both **dOG** and **Fapy-dG** are mutagenic compounds found *in vivo*,[9] while **dOG** is a biomarker monitored to assay the extent of cellular oxidative stress.[21] Because **dOG** has a lower redox potential (0.74 V vs NHE, pH 7; **dOG**•(−H$^+$)/**dOG**) than **dG**,[13] it is readily oxidized to an electrophilic intermediate that reacts with water at C5 to ultimately yield the hydantoin lesions spiroiminodihydantoin-2′-deoxyribonucleoside (**dSp**) and 5-guanidinohydantoin-2′-deoxyribonucleoside (**dGh**).[8,22−25] These lesions have been observed *in vivo* and are also highly mutagentic.[26−29]

Additionally, oxidation of **dG** leads to products resulting from initial chemistry occurring at the C5 position of the purine. 2,5-Diaminoimidazolone-2′-deoxyribonucleoside (**dIz**) and its hydrolysis product 2,2,4-triamino-2*H*-oxazol-5-one-2′-deoxyribonucleoside (**dZ**) are four-electron oxidation products resulting from exposure to HO• or one-electron oxidants under aerobic conditions.[8,18,30−34] Recent studies concerning **dG** oxidation have identified 5-carboxamido-5-formamido-2-iminohydantion-2′-deoxyribonucleoside (**d2Ih**) as a product from Fenton chemistry with copper or lead, activation of $KHSO_5$ with nickel or manganese complexes, $CO_3^{\bullet-}$ oxidations, and the epoxidizing agent dimethyldioxirane.[8,10,35−40] These observations have led us to the question of whether **d2Ih** is in fact a major product from **dG** oxidation by the hydroxyl radical generated either from the Fe(II)-mediated Fenton reaction or by X-ray radiolysis of water.

Toward this goal, we investigated the formation and yield of **dG**-oxidation products from the Fe(II)-mediated Fenton reaction or X-ray radiolysis of water while monitoring the effect of reductant concentration (ascorbate or *N*-acetylcysteine) on their yields in the nucleoside, short oligodeoxynucleotide, and λ-DNA contexts. These studies identify **d2Ih** to be a major guanine oxidation product observed when reactions were conducted with low millimolar amounts of reductant, conditions that mimic the presence of reducing agents such as glutathione, urate, or ascorbate in cells.[41] The results of these studies led to proposed mechanisms for the formation of **d2Ih** and to discussions of its possible biological significance.

RESULTS AND DISCUSSION

Identification of Oxidation Products. The nucleoside **dG** (3 mM) was initially chosen for oxidation by the Fe(II)-mediated Fenton reaction or X-ray irradiation in the absence or presence of ascorbate (Asc) or *N*-acetylcysteine (NAC). All

DOI: 10.1021/acs.joc.5b00689
J. Org. Chem. 2015, 80, 6996−7007

Table 1. Absolute Yields for Oxidation of dG by the Fe(II)-Mediated Fenton Reaction[a]

	absolute yield (%)			
product	Fe(II)/H_2O_2/+Asc/+O_2	Fe(II)/H_2O_2/−Asc/+O_2	Fe(II)/H_2O_2/+Asc/low O_2[b]	Fe(II)/H_2O_2/−Asc/low O_2[b]
dOG	4.9	0.4	6.6	1.9
dSp	5.6	0.9	6.0	3.9
dGh	0.4	<0.1	2.0	1.9
Gh	<0.1	<0.1	N.D.	N.D.
dZ	2.7	1.5	N.D.	N.D.
d2Ih	13.4	0.4	3.3	1.0
cyclo-dG	0.9	0.2	1.9	1.2
Gua	7.1	1.5	N.D.	N.D.
OG	0.6	<0.1	N.D.	N.D.
dG conversion %	35.8	5.0	20.0	9.9

[a]Reported values represent the average of three trials that have errors of ∼8% of the value. N.D. = not detected. [b]Low O_2 represents a partial reduction in the O_2 concentration by bubbling argon into the sample for 10 min that was later found to be insufficient to completely remove O_2.

reactions were conducted with 75 mM NaP_i buffer (pH 7.4) at 22 °C. The reaction mixtures were initially analyzed by reversed-phase UPLC-ESI$^+$-MS. This allowed identification of guanine (**Gua**), 8-oxo-7,8-dihydroguanine (**OG**), **dOG**, and the diastereomers of **cyclo-dG** after comparison to known standards. The void volume from this analysis was collected and reanalyzed with a Hypercarb column equipped with an ESI$^+$-MS detector. This method allowed detection of **Gh**, **dZ**, and the diastereomers of **d2Ih**, **dGh**, and **dSp**. Because **dIz** hydrolyzes to **dZ** during preparation of the void volume, only **dZ** was quantified. The Hypercarb column allowed the separation of the diastereomer products of **d2Ih** and **dSp** for which the absolute configurations for the peaks had been previously determined.[8,42,62] The two diastereomers of **dGh** are interconvertible and were not quantified individually.[44] Further support for the identification of **d2Ih**, **dSp**, and **dZ** was obtained by ESI$^+$-MS/MS fragmentation of the free bases from in-source fragmentation of the *N*-glycosidic bond of the parent nucleosides. The product **dGh** failed to be fragmented. HRMS was conducted to further support the identification of each product (Supporting Information Figures S3−S13).

Product Quantification from the Fe(II)-Mediated Fenton Reaction. Product quantification was conducted with reversed-phase HPLC while monitoring peak elution at 240 nm; product peak areas were integrated and normalized based on the product's extinction coefficient at 240 nm ($\varepsilon_{240\ nm}$).[8] The extinction coefficient for **d2Ih** has not been experimentally determined, and due to its instability toward *N*-glycosidic bond hydrolysis it was not determined in these studies.[43] However, our previous time-dependent density functional theory studies on the UV−vis and ECD properties for **dSp** and **d2Ih** allow us to use these previous results to determine the relative difference in extinction coefficient between these two compounds at the wavelength monitored.[42,43] These calculations determined the $\varepsilon_{240\ nm}$ for **d2Ih** to be ∼30% less than that of **dSp**; therefore, the $\varepsilon_{240\ nm}$ value used to quantify **d2Ih** was calculated to be 2290 $L{\cdot}mol^{-1}{\cdot}cm^{-1}$.[45] The Fenton reaction was initially conducted with the Fe(II)/EDTA catalyst and 10 mM H_2O_2 under aerobic conditions to give 5% conversion to product. We elected to conduct reactions to a low overall yield so that primary oxidation products could be identified and compared. In this reaction, the highest absolute product yields observed were **dZ** (1.5%) and **Gua** (1.5%) in equal amounts, with the mass balance completed by low yields of **cyclo-dG** (0.2%), **dOG** (0.4%), **dSp** (0.9%), and **d2Ih** (0.4%, Table 1). In the next reaction, the same conditions were applied with the addition of 2 mM Asc that led to a 7-fold increase in product formation, as well as a significant change in product distribution. In the presence of Asc, the major **dG** product detected was **d2Ih** (13.4%) with lower yields of the 2-deoxyribose oxidation products **cyclo-dG** (0.9%) and **Gua** (7.1%), as well as **OG** (0.6%) and **Gh** (<0.1%); also, lower yields of **dZ** (2.7%), **dOG** (4.9%), **dSp** (5.6%), and **dGh** (0.4%) were observed (Table 1). These Asc-dependent studies revealed two key observations: (1) the reaction yields dramatically increased (7-fold) with Asc because the Fe(II)/EDTA complex can redox cycle in the presence of a reductant (Reaction 2), and (2) **d2Ih** was the major product observed when Asc was present. Because **dSp** and **dGh** are further oxidation products of the precursor **dOG**,[22] the yield of **d2Ih** (13.4%) was compared to the combined yields of **dOG**, **dSp**, and **dGh** (10.9%), and it was found that the yield of **d2Ih** was higher than that of **dOG** and its oxidation products.

In the next set of reactions, the role of O_2 was studied. First, a reaction was conducted with **dG** in the presence of Fe(II)/EDTA and H_2O_2 under low O_2 conditions achieved by bubbling argon into the sample for 10 min that was insufficient to completely remove O_2. In this reaction, the overall conversion of **dG** to product was 10%, and the major product observed was **dSp** (3.9%), with low yields of **dOG** (1.9%), **dGh** (1.9%), **d2Ih** (1.0%), and the sugar oxidation product **cyclo-dG** (1.2%, Table 1). The addition of 2 mM Asc to the low O_2 reaction increased the **dG** conversion by 2-fold (20%) and changed the product distribution, giving **dOG** (6.6%) and **dSp** (6.0%) in high yield and low yields of **d2Ih** (3.3%), **dGh** (2.0%), and **cyclo-dG** (1.9%, Table 1). These low O_2 studies indicated the yield of **d2Ih** was at a minimum under these conditions. Additionally, the major products observed under low O_2 conditions were **dOG** and its oxidation product **dSp**.

Where is Fapy-dG? Many literature sources point to the presence of **Fapy-dG** as a guanine oxidation product formed under anaerobic, reducing conditions.[46−48] In our present low O_2 studies, this elusive compound was not observed, even after exhaustive searching of the LC-MS data. This led us to probe deeper into the formation of **Fapy-dG**, using the following conditions to make this compound from **dG** by the iron-Fenton reaction. First, the reaction had to be rigorously purged with argon for >30 min prior to addition of H_2O_2 with 2 mM Asc, and the HPLC mobile phase was changed from running

DOI: 10.1021/acs.joc.5b00689
J. Org. Chem. 2015, 80, 6996−7007

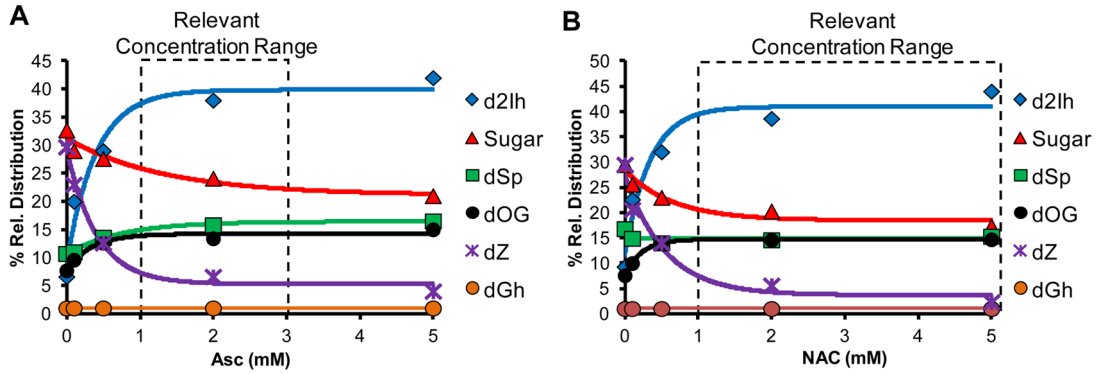

Figure 2. Effect of reductant concentration on relative product distributions observed from the Fe(II)-mediated Fenton reaction. The reactions were conducted with 3 mM **dG**, 10 μM Fe(II)/EDTA, 10 mM H_2O_2 in 75 mM NaP_i buffer (pH 7.4) at 22 °C while varying the concentration of Asc (A) or NAC (B) from 0−5 mM. Data points represent the average of three trials with an error in each value of 3−10%.

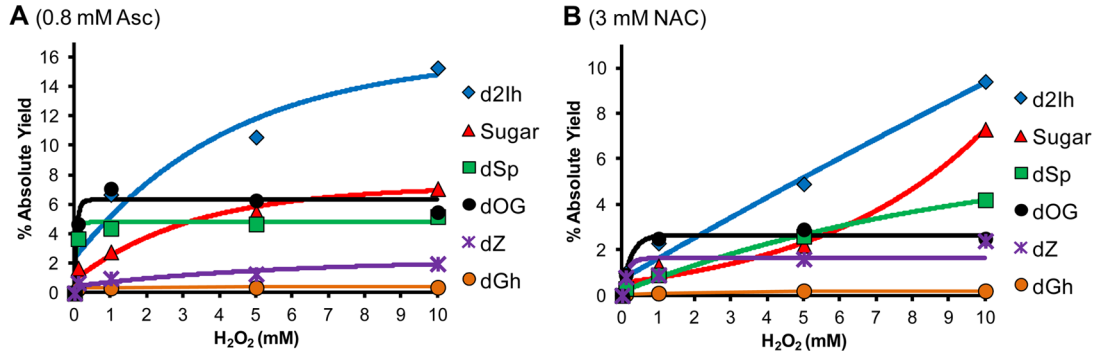

Figure 3. Effect of H_2O_2 concentration on the absolute product distributions from the Fe(II)-Fenton reaction. The reactions were conducted with 3 mM **dG**, 10 μM Fe(II)/EDTA, and with either 0.8 mM Asc (panel A) or 3 mM NAC (panel B) in 75 mM NaP_i (pH 7.4) at 22 °C, while varying the concentration of H_2O_2 from 0−10 mM. Data points represent the average of three trials with an error in each value of 5−11%.

buffered [20 mM NH_4OAc (pH 7)] water and MeCN to unbuffered ddH_2O and MeCN. These changes allowed observation of a broad hump after the void volume in the reversed-phase HPLC chromatogram with a UV−vis signature consistent with **Fapy-dG** (λ_{max} = 270 and 218 nm),[46] and a defined peak that eluted after **dG** with a similar UV−vis profile.[46] The broad hump was consistent with literature reports because **Fapy-dG** exists as anomers of two different sugar configurations.[46,47] LC-ESI$^+$-MS of all these new peaks only found masses consistent with the **Fapy** free base, as well as a peak with mass **Fapy** + 18 (Figure S24). These observations identify that **Fapy-dG** is not stable to laboratory manipulation as are **d2Ih**, **dOG**, **dSp**, or **dGh**, and it appears to be sensitive to nucleophilic buffers in the HPLC mobile phase, e.g., NH_4OAc. Further test reactions that had argon bubbled through them for a few seconds up to 1 min before H_2O_2 addition did not furnish the **Fapy** peaks. The **Fapy** peaks only appeared after purging the system with argon for >30 min. To reiterate, in cases with low O_2 and Asc present, **dOG** was the major product observed, and when O_2 was at ambient concentrations with Asc present, the major product was **d2Ih**. These observations identify **Fapy-dG** to be very challenging to obtain, as it is only observed under extreme anoxic conditions (~100% argon and ~0% O_2), conditions under which cells cannot survive. If **Fapy-dG** was formed in a cell, detection of the nucleoside would be problematic due to the hydrolytic instability of the *N*-glycosidic bond. This later feature is in contrast to **d2Ih**, **dOG**, **dSp**, and **dGh** that are all at least stable enough to allow their characterization under very mild conditions (22 °C in water buffered at pH 7).

Finally, **Fapy-dG** has a low redox potential (1.1 V vs NHE)[47] rendering it subject to further oxidation; however, this is also the case for **dOG** (0.7 V vs NHE)[13] that has an even lower redox potential, and we detect and quantify this intermediate species and its further oxidation products **dSp** and **dGh**. Thus, the conditions outlined do not simply over-oxidize **Fapy-dG** causing its loss. We conclude that **Fapy-dG** is not a major contributor to the product distribution of guanosine oxidation by a hydroxyl radical under cellularly relevant conditions.

Reducing-Agent-Dependent Studies for the Iron-Mediated Fenton Reaction. In cells, two main small-molecule reductants are found in high concentrations, ascorbate and glutathione, found at concentrations of 0.8−3 mM and 1−10 mM, respectively.[41] Knowing that **d2Ih** yields increased when Asc was present during the Fe(II)-mediated Fenton oxidation of **dG** (Table 1), we then studied the role of increasing reductant concentrations on the relative yields of the products. In addition, the nature of the reductant was studied, in which we chose *N*-acetylcysteine (NAC) as a model for glutathione. Note that protection of the amine group of cysteine with an acetyl group prevents amine adduct formation with **dG** oxidation intermediates.[49,50]

Titration of Asc from 0−5 mM into the Fe(II)-mediated Fenton oxidation of **dG** provided the following trends in the relative product distributions (Figure 2A): (1) As the Asc concentration increased, the reaction yield increased, supporting the role of Asc in allowing the iron catalyst to redox cycle

DOI: 10.1021/acs.joc.5b00689
J. Org. Chem. 2015, 80, 6996−7007

between Fe(II) and Fe(III) and thereby increasing the production of HO• (Reactions 1 and 2). (2) The amount of 2-deoxyribose oxidation decreased (~10%) as the concentration of Asc increased. This observation negates the involvement of Asc in sugar oxidation, and it is likely that Asc inhibits this pathway. (3) The relative yields of **dOG**, **dSp**, and **dGh** slightly increased (~6%) with more Asc. (4) The Asc concentration was shown to be critical in the relative yields of the C5 products, **dZ** and **d2Ih**. When Asc was not present, the major C5-oxidation product was **dZ** (also a major product overall); however, as Asc was titrated into the reaction, the relative yield of **dZ** decreased and **d2Ih** increased until it was the major product of the reaction at Asc >2 mM (Figure 2A). Within the range of physiological Asc concentrations (1−3 mM),[41] **d2Ih** was always the major oxidation product detected (Figure 2A). Moreover, when the study was conducted with variable NAC concentrations, the same trends were observed (Figure 2B). Again, the most notable observation is that **d2Ih** was the major oxidation product observed in reactions conducted with >2 mM thiol concentrations (Figure 2B), even when considering a comparison of **d2Ih** (~37%) with the combined yields of **dOG**, **dSp**, and **dGh** (~30%, Figure 2A and 2B with 2 mM reductant).

H_2O_2 Concentration-Dependent Studies for the Iron-Mediated Fenton Reaction. In the next set of studies, **dG** oxidation product distribution versus the H_2O_2 concentration (0−10 mM) was monitored with a static amount of reductant (0.8 mM Asc or 3 mM NAC, Figure 3A and 3B, respectively). Key observations from these studies include the following: (1) As expected, the reaction yield increased as more H_2O_2 was added to the reaction (Supporting Information, Figures S16 and S17). (2) With increased H_2O_2 concentrations, the flux of HO• increased, and the relative yield of **dSp** increased at the expense of **dOG**. This observation supports **dOG** as the intermediate leading to **dSp**.[10,11] (3) Both **dZ** and **d2Ih** increased as a function of H_2O_2 concentration (0−10 mM); moreover, the amount of **d2Ih** increased 4-fold when Asc was the reductant while **dZ** increased 3-fold (Figure 3A). In the H_2O_2-dependent studies with NAC, **d2Ih** increased 13-fold while **dZ** increased 3-fold when H_2O_2 increased from 0 to 10 mM (Figure 3B). These studies demonstrate that the yield of **d2Ih** was maximal under conditions that boost formation of HO•.

Product Quantification from X-ray-Mediated Oxidation of dG. Next, oxidation of **dG** was conducted with an X-ray source at a dose rate of 25 Gy/min for 30 min (total dose = 750 Gy). Initial studies without a reductant gave a 45% conversion of **dG** to product. The major oxidation products observed were **dZ** (14.7%), **dSp** (10.8%), and **Gua** (12.4%) and in low absolute yields were **d2Ih** (2.9%), **dOG** (1.4%), and **dGh** (1.4%). Next, Asc (2 mM) was added to the reaction to give the following changes in the yields. (1) The absolute conversion of **dG** to product decreased with Asc (2.5-fold), as expected, because Asc quenches radical reactions.[51] (2) The major products were now **d2Ih** (6.3%), **dSp** (3.9%), and **Gua** (4.1%), with the mass balance completed by low yields of **dZ** (1.1%), **dOG** (2.5%), **cyclo-dG** (0.5%), and **dGh** (<0.1%). The most striking observation was that **d2Ih** was the major oxidation product when Asc was present during X-ray mediated oxidations; however, this is in contrast to studies without Asc where **dZ** was the major oxidation product quantified (Table 2). When considering the yield of **d2Ih** (6.3%) in comparison to the combined yields of **dOG**, **dSp**, and **dGh** (6.4%), the initial split between **d2Ih** and the C8 products was nearly equal with X-ray irradiation when reductant was present. Because the X-ray reactions required the reaction vessel to be open to the atmosphere, studies were not conducted under anaerobic conditions.

Table 2. Absolute Yields for Oxidation of dG by X-ray Radiolysis of Water[a]

	Absolute Yield (%)	
product	X-ray +Asc/+O_2	X-ray −Asc/+O_2
dOG	2.5	1.4
dSp	3.9	10.8
dGh	0.2	1.4
Gh	<0.1	0.5
dZ	1.1	14.7
d2Ih	6.3	2.9
cyclo-dG	0.5	0.1
Gua	4.1	12.4
OG	0.2	N.D.
dG conversion %	18.8	45.3

[a]Reported values represent the average of three trials, and the error in each value was 4−10%. N.D. = not detected.

Reducing-Agent-Dependent Studies for the X-ray Mediated Oxidations. Reactions with and without Asc suggest a major role for the reductant in the product distributions for X-ray mediated oxidations (Table 2). Therefore, studies were conducted with the reductant Asc or NAC titrated (0−5 mM) into the X-ray-mediated reaction mixture while monitoring the product yields (Figure 4A and 4B). From these studies, the following observations were made in X-ray-mediated oxidations: (1) As the reducing agent concentration increased, the reaction yield significantly decreased (Supporting Information, Figures S19 and S21). (2) The relative yield of **dOG** increased (6-fold) as a function of reductant concentration (Figure 4A and 4B), while the yield of **dSp** decreased (1.5-fold) and **dGh** decreased (3-fold). This result supports the conclusion that the reductant quenched the further oxidation of **dOG** to the hydantoins. (3) The yields of the sugar oxidation products were not significantly changed by the increase in reductant concentration (Figure 4A and 4B). (4) The reductant had the most dramatic effect on the C5-pathway products, **dZ** and **d2Ih**. When the reductant was not present, **dZ** was the major product and **d2Ih** was observed in very low yield; however, when Asc or NAC was increased to relevant concentrations, **d2Ih** was the major oxidation product observed with very little **dZ** detected.

Total X-ray Dose Effect on dG Oxidation Product Distributions. In the next set of reactions, **dG** was irradiated with X-rays at a rate of 25 Gy/min while varying the time (i.e., total dose) and keeping the Asc concentration static (2 mM). As the total dose of X-rays increased from 25 to 750 Gy, the following trends were observed. (1) As expected, the overall reaction yield increased (Supporting Information Figure S22). (2) The yield of **dSp** and **dGh** increased at the expense of **dOG** with increasing X-ray dose. (3) The yield of sugar chemistry increased with increasing X-ray dose. (4) The yield of **dZ** and **d2Ih** both increased as a function of the X-ray dose, and **d2Ih** was always the major C5-oxidation pathway product, as well as being the major product of the reaction overall (Figure 5).

Proposed Pathways Leading to dG Oxidation Products. Under all of the conditions studied, products derived

DOI: 10.1021/acs.joc.5b00689
J. Org. Chem. 2015, 80, 6996−7007

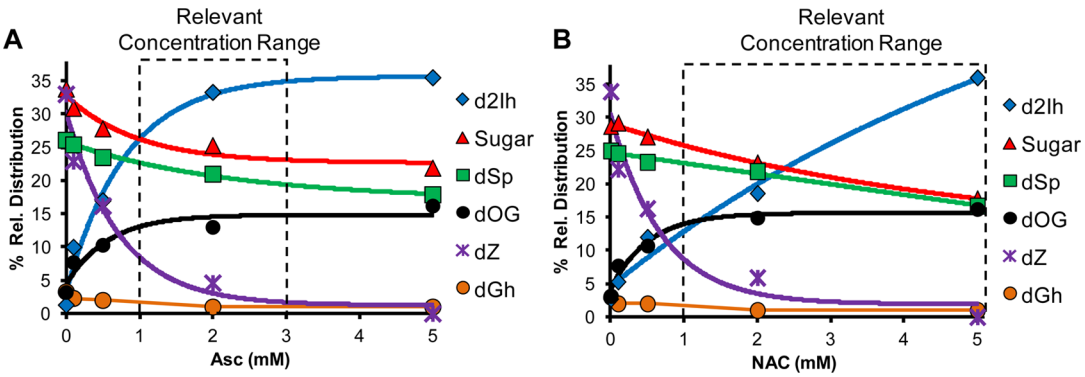

Figure 4. Effect of reductant concentration on the **dG**-oxidation product yield from the X-ray reaction. The reactions were conducted with 3 mM **dG** in 75 mM NaP_i (pH 7.4) at 22 °C with a 30 min exposure to 25 Gy/min X-ray source (total dose = 750 Gy) while varying the concentration of Asc (panel A) or NAC (panel B) from 0−5 mM. Data points represent the average of three trials with an error in each value of 3−10%.

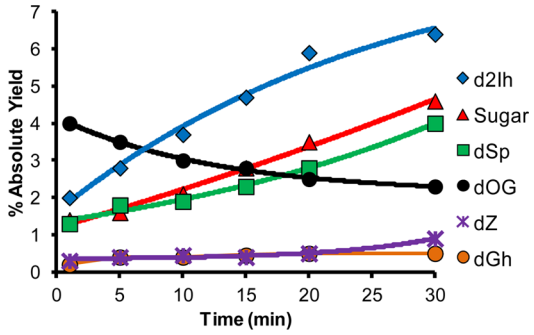

Figure 5. Effect of X-ray irradiation time on **dG**-oxidation product distributions. The reactions were conducted with 3 mM **dG**, 2 mM Asc in 75 mM NaP_i (pH 7.4) at 22 °C while varying the exposure time (0−30 min) to an X-ray source that was delivered at a rate of 25 Gy/min. Data points represent the average of three trials with an error in each value of 3−10%.

from sugar oxidation were observed. Oxidation at the 5′-carbon yields the 5′ carbon-centered radical that attacks C8 of the heterocyclic ring of **dG** to furnish an intermediate radical that loses another electron and proton to furnish **cyclo-dG** (Scheme 1). Oxidation at the 1′, 2′, 3′, 4′, or 5′ carbons also yields a carbon-centered radical that reacts with O_2, and many of these pathways ultimately cause cleavage of the *N*-glycosidic bond releasing **Gua** (Scheme 1).[12,15] Evidence of these sugar oxidation pathways was determined by quantification of **Gua** release. The yield of **cyclo-dG** in the Fenton reaction was maximal under anaerobic reducing conditions and was observed to be at a minimum under aerobic nonreducing conditions (Table 1). In contrast, base release to give **Gua** was observed to be maximal under aerobic and reducing conditions and not observable under anaerobic conditions (Table 1). These results further support the role of O_2 in effecting base release from 2-deoxyribose oxidation.[12] Moreover, this reaction was not sensitive to the presence of the reductant. However, under anaerobic conditions the 5′-carbon radical was not trapped by

Scheme 1. Proposed Pathway for Products Derived from Sugar Oxidation[a]

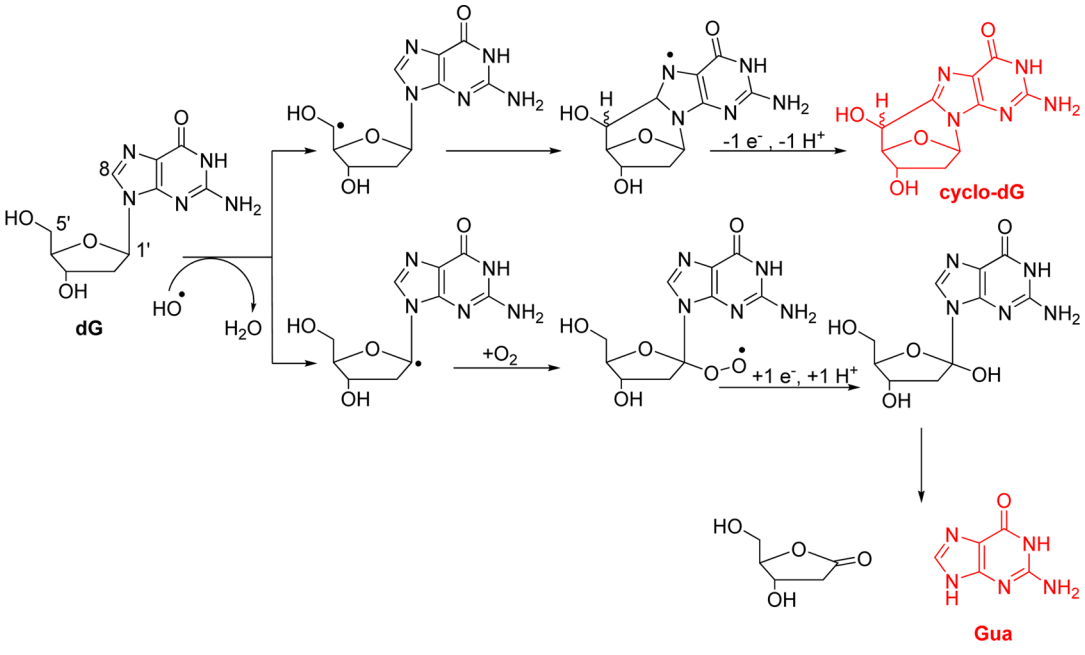

[a]For the sake of brevity, only oxidation of the 1′-carbon leading to **Gua** is shown.

DOI: 10.1021/acs.joc.5b00689
J. Org. Chem. 2015, 80, 6996−7007

O_2, but rather added into the heterocyclic ring at C8 leading to **cyclo-dG**, and again this reaction was not sensitive to the presence of the reductant. Also observed in very low yield were **OG** and **Gh**, two products that are derived from further oxidation of **Gua** (Table 1). The observation of **Gh** and not **Sp** under these conditions (pH 7.4 and 22 °C) is consistent with a previous observation that oxidations of the free base **OG** only give **Gh** and not **Sp**.[52] In the X-ray-mediated oxidation of **dG**, O_2-dependent studies could not be conducted; therefore, only product dependence on the reductant was studied. In this study, the products derived from sugar oxidation were not greatly affected by the presence of the reductant (Table 2). Other products resulting from oxidation of the 2-deoxyribose sugar in **dG** were not observed by LC-ESI$^+$-MS (Figure S3).

Oxidation of **dG** at the C8 position yields **dOG** and **Fapy-dG**.[4,10] Mechanistically, these products form when HO$^\bullet$ adds at the C8 carbon to yield **8-HO-dG**$^\bullet$ (Scheme 2). This

Scheme 2. HO$^\bullet$-Mediated Oxidation of dG at C8 Leading to dOG and Fapy-dG

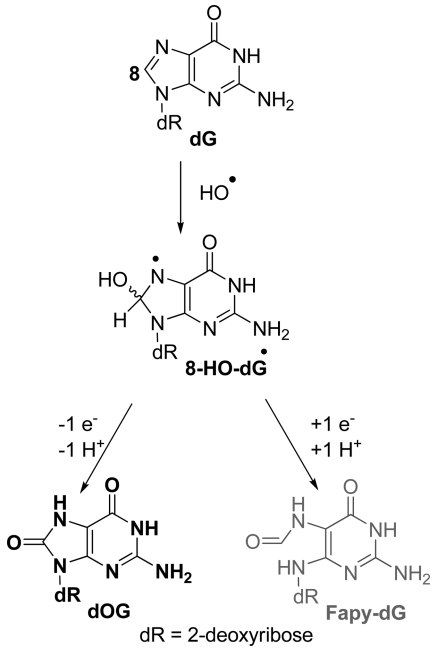

intermediate can be further oxidized to yield **dOG**, or be reduced and ring opened to yield **Fapy-dG** (Scheme 2).[4,10] Under all conditions, **dOG** was observed; however, we did not detect **Fapy-dG** in these studies without exhaustive removal of O_2 (Figure S24). In both the Fenton and X-ray oxidations, the yield of **dOG** was at a maximum when the reductant was present, which appears to be inconsistent with previous results;[20] however, the current studies were conducted under aerobic conditions (Tables 1 and 2), while the previous studies were conducted under anaerobic conditions. Because **dOG** can undergo further oxidation to hydantoin products (see below),[22] the presence of the reductant suppresses the further oxidation and addresses why **dOG** concentrations are highest under oxidations conducted with the reductant. In conclusion, HO$^\bullet$-mediated oxidation of **dG** via Fe(II)-Fenton chemistry and X-ray irradiation effects oxidation at C8 of **dG** to yield **dOG** as the dominant product along this pathway under low oxidant flux with O_2 and the reductant present (Figures 3A, 3B, and 5). Furthermore, as the oxidant flux increases, the yield of **dOG** decreases due to further oxidation to **dSp**.

The low redox potential of **dOG** renders this nucleoside labile toward further oxidation to yield the hydantoins **dSp** and **dGh** (Scheme 3).[22,54] Two-electron oxidation of **dOG** followed

Scheme 3. Proposed Pathway for Products Derived from Further Oxidation of dOG

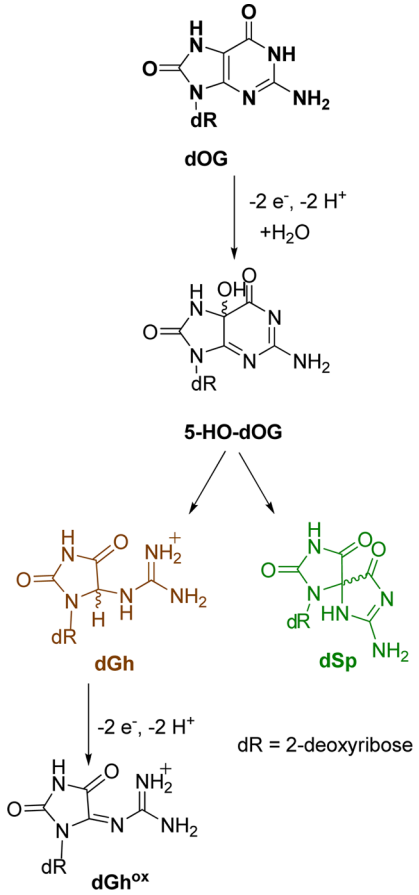

by water attack at C5 yields **5-HO-dOG** that bifurcates along two pathways to either **dSp** or **dGh**.[22,43,44,54] Acyl migration to **dSp** dominates under conditions of higher pH (pH > 5.8) and unencumbered contexts such as nucleosides, single-stranded DNA, and G-quadruplexes, while the yield of **dGh** is highest at low pH (pH < 5.8) or sterically encumbered contexts such as double-stranded DNA.[22,43,44,54,55] These and previous observations explain why **dSp** was the major hydantoin observed in all unencumbered nucleoside studies. As previously stated, the yield of **dOG** was highest when the reductant was present at relevant concentrations (Figures 2 and 4). In contrast, the yield of **dSp** was highest in the absence of the reductant. This observation supports **dOG** being the stable intermediate that leads to **dSp**, as further oxidation of **dOG** to **dSp** was quenched with added reductant (Figures 2 and 4). These data, in which **dOG** was obtained in greater yield than the hydantoins under conditions with physiologically relevant reductant, further explain why concentrations of **dOG** are generally much greater than hydantoins *in vivo*.[26,56]

Oxidations of **dOG** have detected a four-electron oxidation product dehydroguanidinohydantoin-2′-deoxyribonucleoside (**dGh^{ox}**), or formally a six-electron oxidation product of **dG** (Scheme 3).[57] This compound has a short half-life and

DOI: 10.1021/acs.joc.5b00689
J. Org. Chem. 2015, 80, 6996−7007

Scheme 4. Proposed Pathway for Oxidation of dG Followed by Initial Reaction at C5 Leading to dZ

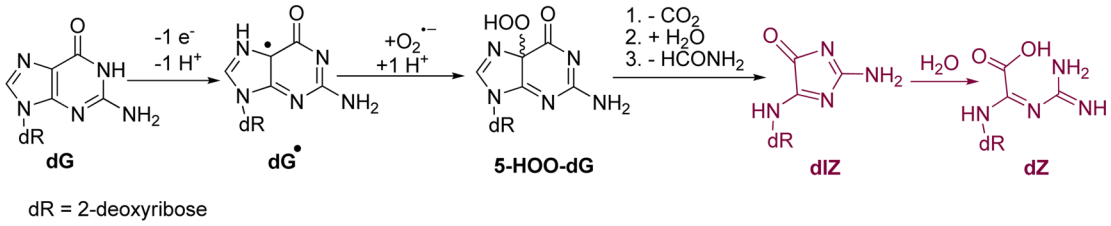

Scheme 5. Proposed Pathways for d2Ih Product Derived from C5 Pathway Oxidation

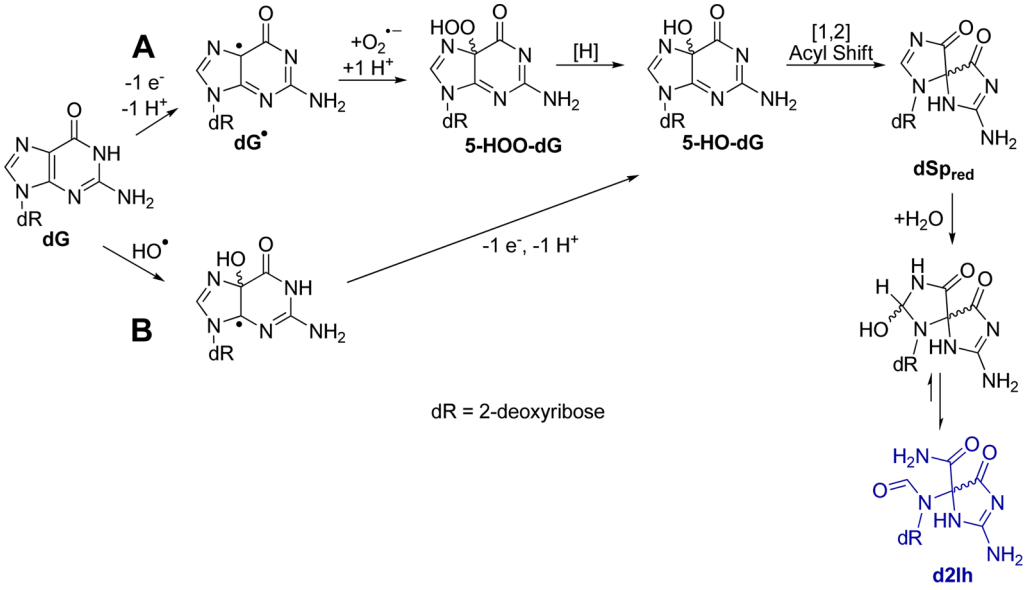

decomposes to yield oxaluric acid that further hydrolyzes to liberate oxalate and ultimately 2′-deoxyribosyl-urea.[58] These analytical conditions allow identification of oxaluric acid (unpublished result from our laboratory); however, under the current HO•-mediated oxidations, neither **dGh^{ox}** nor oxaluric acid were detected. In these studies, low product conversion was maintained, preventing hyperoxidation of **dG** to **dGh^{ox}**.

The products **dZ** and **d2Ih** result from oxidation of **dG** followed by initial product forming chemistry occurring at C5. Previous HO•-mediated oxidations of **dG** detected **dZ** as a major product under aerobic and nonreducing conditions, which we observed in these studies (Tables 1 and 2).[59,60] Mechanistically, **dZ** was proposed to form from one-electron oxidation of **dG** (**dG$^{•+}$**/**dG$^{•}$**$(-H^+)$, pK_a ∼3.9)[55] to a neutral radical that couples with $O_2/O_2^{•-}$ to ultimately yield a hydroperoxy intermediate (**5-HOO-dG**). Next, **5-HOO-dG** decomposes through a multistep process to **dIz** followed by hydration to **dZ** (Scheme 4).[54,56,57] Additional support for the role of $O_2/O_2^{•-}$ in the product defining step leading to **dZ** was observed in the reactions under anaerobic conditions, for which **dZ** was not detected (Table 1). Further, as the reducing agent was titrated into the reactions, the yield of **dZ** dramatically decreased, an observation consistent with a previous report.[59]

When the oxidations were conducted under aerobic conditions with relevant concentrations of the reductant (Asc or NAC), **d2Ih** was the major product detected (Figures 3, 4, and 5). In Scheme 5 a mechanism is proposed to explain this observation. Formation of HO• via the Fe(II)-Fenton reaction or X-ray radiolysis of water (Reactions 1 − 4) effects the one-electron oxidation of **dG** followed by proton loss to yield **dG•**. Next, **dG•** couples with $O_2^{•-}$ to ultimately yield **5-HOO-dG**[24] that is the intermediate susceptible to reduction. When the reductant was not present, **5-HOO-dG** decomposes to yield **dIz**; however, when the reductant was present, the hydroperoxyl group can be reduced to the alcohol **5-HO-dG**. Next, **5-HO-dG** undergoes acyl migration to **reduced-dSp** (**dSp$_{red}$**) that hydrates at C8 and ring opens to yield **d2Ih** (Scheme 5A). This proposed mechanism provides a role for O_2 and the reducing agent in the formation of **d2Ih** that was observed in the product distribution studies (Figures 2 and 4). The proposed mechanistic steps from **5-HO-dG** to **d2Ih** were previously proposed from **dG** oxidations with $KHSO_5$ catalyzed by a Mn−porphyrin complex.[36,61]

Because **d2Ih** was also observed under anaerobic conditions (Table 1) there must be an alternative pathway for its formation that is not O_2 dependent. In Scheme 5B, such a mechanism is proposed in which HO• adds to C5 yielding **5-HO-dG•** that proceeds through a second one-electron oxidation and deprotonation to yield **5-HO-dG**; acyl migration and hydration then yield **d2Ih** (Scheme 5B). This second pathway provides a route to **d2Ih** under anaerobic and nonreducing reaction conditions. The alternative pathway must be a minor reaction channel to **d2Ih**, because added reductant significantly increases **d2Ih** formation supporting the mechanism in Scheme 5A.

Product formation upon oxidation of **dG** initially occurs on the sugar leading to base release or **cyclo-dG** (Scheme 1), on C5 of the heterocyclic base leading to **d2Ih** and **dZ** (Schemes 4 and 5), or on C8 of the heterocyclic base leading to **Fapy-dG** and **dOG** (Scheme 2), in which **dOG** is further oxidized to **dSp**

DOI: 10.1021/acs.joc.5b00689
J. Org. Chem. 2015, 80, 6996−7007

and **dGh** (Scheme 3). Inspection of the product distributions allows ranking the initial **dG** site of reactivity toward oxidation under each condition. The focus will be on reactions conducted under aerobic conditions with and without the addition of Asc (Tables 1 and 2). The iron-Fenton reaction without the addition of Asc focused on the sugar, C5, and C8 carbons in a ratio of 1.3:1.5:1.0, respectively, with the C5 products showing the highest yield. A comparison of the C5 and C8 product distributions show that C5 products are ∼150% of the C8 products. When Asc (2 mM) was added to the mixture, the ratio of reactivity was 1.0:1.9:1.3 for the sugar, C5, and C8 carbons, respectively (Table 1). The addition of Asc to the iron-Fenton reaction suppressed oxidation of the sugar, and initial reaction at the C5 was still greater than C8. More interestingly, C5 products were still ∼150% more than the C8 products. This observation is consistent with the proposed mechanistic role of Asc in product formation, in which it reduces intermediate species that have already reacted at C5 or C8 (Scheme 5).

The X-ray mediated oxidation of **dG** without Asc yielded sugar, C5, and C8 products in a 1.0:1.4:1.0 ratio, respectively (Table 2). Initial reactivity at C5 was the dominant pathway, and it was ∼140% greater than the C8 pathway, similar to that observed for the iron-Fenton mediated oxidation of **dG**. When Asc was added to the mixture the ratio of reactivity at the sugar, C5, and C8 sites on dG was 1.0:1.5:1.4, respectively. Overall, Asc decreased the sugar oxidation products (Table 2) and the C5 and C8 products were found in nearly the same yield. The reason C5 and C8 products were observed in similar yields has to do with **dZ**. The presence of Asc dramatically diminished the yield of **dZ** in the X-ray mediated oxidations, leading to less C5 products and similar yields of C5 and C8 products. These comparisons support a greater level of oxidation occurring at the heterocyclic ring of the **dG** nucleoside compared to the sugar particularly with Asc present.

Use of a Hypercarb column allowed separation of the **d2Ih** and **dSp** diastereomers for which the absolute configurations and elution order on this HPLC column are known.[42,62] In the current studies, the *R* and *S* isomers of **d2Ih** were observed in a 1:2 ratio, respectively, for both oxidation reactions studied, while the *R* and *S* isomers of **dSp** were observed in a 1:1 ratio. Furthermore, these ratios did not change under any of the reaction conditions studied. The observation that the **d2Ih** isomers were not in a 1:1 ratio points to steric hindrance during the defining point of the reaction that determines product stereochemistry and was likely caused by the 2-deoxyribose sugar. In contrast to this result, the diastereomer ratio of **d2Ih** found from the copper-mediated Fenton oxidation was 2:1.[8] In the other **d2Ih** studies, the diastereomer identity and ratios were not stated.[35,36,38−40]

In the last study, the products resulting from base oxidation of **dG** in oligonucleotides of known sequence in single- (ODN1) and double-stranded (ODN2) contexts were determined, as well as products observed from λ-DNA. The product analysis was achieved using HF to hydrolyze the bases from the sugar−phosphate backbone. This approach prevented the quantification of sugar oxidation leading to base release. Because of this limitation, only base oxidation products are compared. Further, products resulting from oxidation of other nucleotides, leading to thymine glycol, for example, were observed but were not quantified; masses consistent with guanine cross-links with thymine and cytosine were observed, but their yields are not reported due to a lack of established extinction coefficients to obtain their yields (Figure S24). These limitations in product analysis prevent an ideal comparison; however, we can use these data to understand context-dependent product distributions leading to C5 products (**2Ih** and **Z**) vs C8 products (**OG**, **Sp**, and **Gh**) when iron-Fenton or X-ray mediated oxidations were conducted with Asc (2 mM) present under aerobic reaction conditions.

5′-TCA TCG GTC GTC GGT ATA-3′ ODN1

5′-TCA TCG GTC GTC GGT ATA-3′ ODN2
3′-AGT AGC CAG CAG CCA TAT-5′

The overall context-dependent trends were very similar for iron-Fenton and X-ray irradiation reactions (Figure 6 A and B).

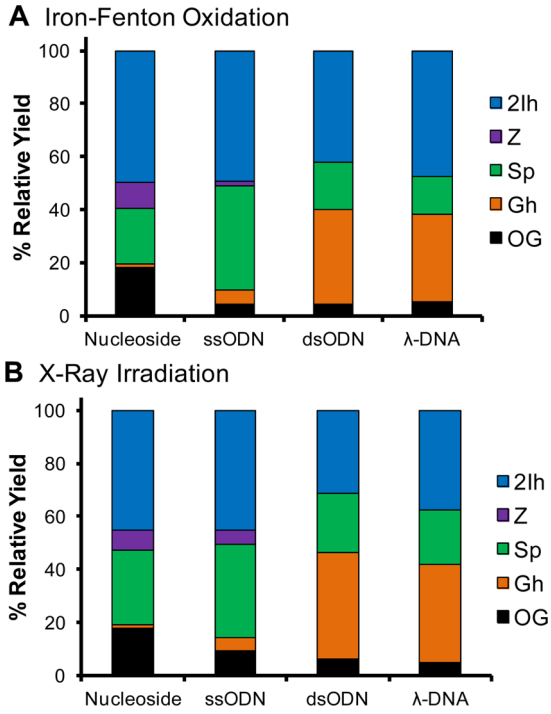

Figure 6. Context-dependent yields of dG base oxidation products from the iron-Fenton and X-ray irradiated samples. The ODN and λ-DNA distributions were obtained after HF hydrolysis of the oxidized samples. In the ODN and λ-DNA samples, products were also observed from oxidation of the other nucleotides. Because of the HF hydrolysis to liberate the oxidized free bases, the extent of sugar oxidation leading to free base could not be determined.

The relative yield of **Z** diminished dramatically when comparing oxidations between nucleoside to ODN and DNA contexts. In the duplex contexts no **Z** was observed, an observation similar to previous studies of the added reductant during the oxidations.[52] The **OG** free base was observed in all contexts and comprised the smallest relative yield in the ODN and DNA contexts and largest yield in the nucleoside studies from both iron-Fenton and X-ray oxidations. The yield of **Sp** and **Gh** showed strong context-dependent yields, in which **Sp** was greatest in nucleoside and single-stranded contexts and **Gh** was observed to be greatest in duplex contexts. This observation is consistent with previous reports.[8,43] Lastly, the relative yield of **2Ih** remained nearly the same in all three contexts (∼40−50%, Figure 6A and B). Without complete mass balances for oxidations in the ODN and DNA contexts, it

DOI: 10.1021/acs.joc.5b00689
J. Org. Chem. 2015, 80, 6996−7007

Table 3. Comparison of the Current Results to Other Reports[a]

	initial reaction at C8		initial reaction at C5		initial reaction at 2-deoxyribose	
	products					
oxidants	dOG	dSp/dGh	dIz/dZ	d2Ih	sugar	reference
HO• (radiolysis)	+	+	++	N.D.	+	59,60
$CO_3^{\bullet-}$	+	+	+	++	+	39
Pb(II)/H_2O_2	+	+	+	++	+	40
NiCR/$KHSO_5$	N.D.	+	N.D.	++	N.D.	35
DMDO	N.D.	N.D.	N.D.	++	N.D.	37
Cu(I)/H_2O_2	+	+	+	++	+	8
Dicopper(II)-complex	N.D.	N.D.	N.D.	++	N.D.	64
Mn-TMPyP/$KHSO_5$	N.D.	+	+	++	+	61
Fe(II)-EDTA/H_2O_2/Asc or NAC	+	+	+	++	+	current study
X-ray/Asc or NAC	+	+	+	++	+	current study

[a](++) a major product, (+) a minor product, (N.D.) not detected or not reported.

cannot be definitively stated that **d2Ih** is the major oxidation product of **dG**; nonetheless, **d2Ih** is clearly a major product observed from oxidation of **dG** in the nucleoside, single- and double-stranded ODN, and λ-DNA contexts. This observation supports the possibility of **d2Ih** formation in the cellular context.

The current results are compared to literature studies that reported **d2Ih** as shown in Table 3. The Ball laboratory exclusively observed **d2Ih** when **dG** was exposed to the epoxidizing reagent dimethyldioxirane (DMDO), and they confirmed the structure of **d2Ih** via complementary NMR methods.[37,63] The Meunier laboratory observed **d2Ih** (**M+34**) when **dG** was oxidized with Mn-TMPyP/$KHSO_5$.[36,61] Studies in the Karlin and Rokita laboratories observed a product mass in high yield consistent with **d2Ih** (**M+34**) when an oligodeoxynucleotide was allowed to react with a dicopper-(II)-complex.[38,64] In our laboratory, **d2Ih** was detected in high yield with the NiCR/$KHSO_5$ system, and in studies utilizing the copper-mediated Fenton oxidation of **dG**.[8,35] Further, the Bohme laboratory conducted the lead-mediated Fenton oxidation of **dG** to yield **d2Ih** as the major product.[40] In all of the metal-catalyzed studies, the transition metal was proposed to play a role in the product-forming step leading to **d2Ih**. However, studies conducted in the Shafirovich laboratory observed **d2Ih** during $CO_3^{\bullet-}$ oxidations of **dG**, demonstrating that a transition metal was not required for **d2Ih** formation.[39] In the current report, **d2Ih** was the major product of "free" HO•-mediated oxidation of **dG** with relevant amounts of reductant under aerobic conditions. The X-ray studies demonstrate once again that **d2Ih** can be formed under conditions that do not require the involvement of a transition-metal catalyst.

CONCLUSIONS

The current studies monitored oxidation products from **dG** resulting from HO• generated via the Fe(II)-mediated Fenton reaction or X-ray radiolysis of water. Products resulting from oxidation and initial reaction at the sugar, C5, or C8 carbons were quantified (Figures 2−5). Under aerobic conditions without a reductant, the major products observed include **dZ**, **dSp**, and sugar oxidation leading to **Gua**. Under anaerobic reaction conditions the major product observed was **dSp**. When reactions were conducted with cellularly relevant (mM) amounts of the reductant (Asc or NAC) and O_2, the major product observed in all cases was **d2Ih**. The isomers of **d2Ih** are two-electron oxidation products of **dG** that have not been previously detected in oxidations with HO• generated by the Fe(II)-mediated Fenton reaction or X-ray radiolysis of H_2O. The high yields of **d2Ih** observed and the observation that this lesion is highly prone to piperidine cleavage in a DNA oligomer, unlike **dOG**,[65] lead to a hypothesis that oxidations in DNA imposed by electron transfer agents yield C5 oxidation products (i.e., **d2Ih** or **dZ**) and not the C8 oxidation product **dOG**.[66] Oxidations in the context of single- and double-stranded ODNs and λ-DNA yielded **d2Ih** as a product of **dG** oxidation in significant yield that was competitive with the yield of **dOG**. More importantly, the current results highlight **d2Ih** as a major product observed in reactions that include relevant amounts of reductant in the presence of O_2, suggesting that **d2Ih** should be investigated more closely for its biochemical properties.

EXPERIMENTAL PROCEDURES

Fenton Reaction. A 200-μL solution of **dG** (3.0 mM, 0.6 μmoles, 0.16 mg) in a buffer (75.0 mM NaP_i, pH 7.4) was mixed with Fe(II)/EDTA (0.10 mM, 0.02 μmoles, 0.008 mg), H_2O_2 (10.0 mM, 2 μmoles, 0.5 mg), and Asc or NAC (2.0 mM, 0.40 μmoles, 0.03 mg) and incubated for 1 h at 22 °C. The Fe(II)/EDTA complex was freshly made by mixing $Fe(NH_4)_2(SO_4)_2$ and Na_2EDTA in a 1:2 ratio 30 min prior to reaction. The Fe(II)/EDTA complex was removed by column chromatography using ion-exchange resin prior to HPLC analysis following the method outlined below.

X-ray Irradiation. A 200-μL solution containing **dG** (3.0 mM, 0.6 μmoles, 0.16 mg) in buffer (75.0 mM NaP_i, pH 7.4) and Asc or NAC (2.0 mM, 0.40 μmoles, 0.03 mg) was irradiated with an X-ray RS 2000 biological research irradiator source at 22 °C for variable times (1−30 min). The dose rate was 25 Gy/min.[59] This solution was analyzed by the method outlined below.

Oligodeoxynucleotide and DNA Oxidations. Single-stranded ODN1 or double-stranded ODN2 were oxidized in 20 mM NaP_i (pH 7.4) with 100 mM NaCl at 37 °C. Iron-Fenton oxidations were conducted in a 200-μL reaction volume with ODN (100 μM, 0.01 μmoles, 0.05 mg) to which were added Fe(II)EDTA (0.10 mM, 0.02 μmoles, 0.008 mg), Asc (2.0 mM, 0.40 μmoles, 0.03 mg), and H_2O_2 (1.0 mM, 0.2 μmoles, 0.05 mg); the reaction was allowed to proceed for 30 min. The stock solutions of Fe(II)EDTA, Asc, and H_2O_2 were all freshly prepared. To irradiate the ODNs, they were placed in the same buffer system as the iron-Fenton reaction followed by X-ray irradiation with a dose rate of 25 Gy/min for 30 min (total dose = 750 Gy). For the λ-DNA oxidations, everything was identical to the ODN oxidations with the exception that the λ-DNA (1 μM, 0.1 nmol, 0.03 mg) was different.

DOI: 10.1021/acs.joc.5b00689
J. Org. Chem. 2015, 80, 6996−7007

Hydrolysis of Oxidized Oligodeoxynucleotides and λ-DNA. The oxidized ODN or λ-DNA samples were hydrolyzed to the free bases for HPLC analysis. The hydrolysis was performed on the oxidized and lyophilized DNA by adding 50 μL of 70% HF in pyridine for 30 min at 37 °C. After the reaction, the excess HF was neutralized by adding 1 mL of ddH_2O and 80 mg of $CaCO_3$ to the sample. The insoluble salts were removed by centrifugation, and the supernatant was then lyophilized to dryness. Next, the lyophilized samples were dissolved in ddH_2O and submitted to LC-MS and HPLC analysis as described for the nucleoside studies below.

Product Identification. Product identification was initially achieved by UPLC-ESI$^+$-MS (100 mm × 2.1 mm, 1.7 μm) and UPLC-ESI+-MS with a Hypercarb column (100 mm × 2.1 mm, 5 μm). Then, each compound was HPLC purified for further structural analysis. The following masses were observed: **Gua** m/z $[M + H]^+$ calcd 152.1, found 152.1. **OG** m/z $[M + H]^+$ calcd 168.1, found 168.1. **dOG** m/z $[M + H]^+$ calcd 284.2, found 284.1. *R* and *S* diastereomers of **cyclo-dG** m/z $[M + H]^+$ calcd 266.2, found 266.1. **Gh** m/z $[M + H]^+$ calcd 158.1, found 158.1. **(*S*)-d2Ih** and **(*R*)-d2Ih**[42] m/z $[M + H]^+$ calcd 302.3, found 302.1; ESI$^+$-MS/MS m/z $[M + H]^+$ lit.[37] 186, 158, and 141; found 186, 158, and 141. HRMS (ESI-TOF) m/z $[M + Na]^+$ calcd for $C_5H_7N_5O_3Na$ 208.0447, found 208.0449. The HRMS value was obtained on the free base **2Ih**, due to the nucleoside's instability toward acid. **dGh** m/z $[M + H]^+$ calcd 274.3, found 274.1; HRMS (ESI-TOF) m/z $[M + Na]^+$ calcd for $C_9H_{15}N_5O_5Na$ 296.0971, found 296.0980. **(*S*)-dSp** and **(*R*)-dSp**[62] m/z $[M + H]^+$ calcd 300.2, found 300.1; HRMS (ESI-TOF) m/z $[M + Na]^+$ calcd for $C_{10}H_{13}N_5O_6Na$ 322.0764, found 322.0761; ESI$^+$-MS/MS m/z $[M + H]^+$ lit.[22] 184, 156, 141, 113, 99, and 86; found 184, 156, 141, 113, 99, and 86. **dZ** m/z $[M + H]^+$ calcd 247.2, found 247.1; HRMS (ESI-TOF) m/z $[M + Na]^+$ calcd for $C_8H_{14}N_4O_5Na$ 269.0862, found 269.0870; ESI$^+$-MS/MS m/z $[M + H]^+$ lit.[67] 247, 203, and 131; found 247, 203, and 131 (Figures S3−S13, Supporting Information). The **dGh** diastereomers were characterized by NMR,[44] **dZ** was characterized by NMR,[30] **cyclo-dG** was characterized by X-ray crystallography,[68] the **dSp** diastereomers have been characterized by X-ray crystallography[69] and NMR,[70] and the diastereomers of **d2Ih** have been previously characterized by NMR.[37]

Product Quantification. The oxidation products from the Fe(II)-Fenton reaction or X-ray irradiation reaction were quantified by C18 reversed-phase HPLC and Hypercarb HPLC. First, the reaction mixture was injected on a reversed-phase HPLC (250 mm × 4.6 mm, 5 μm) to quantify **Gua**, **OG**, **dOG**, and **cyclo-dG**. The void volume from this run was collected, lyophilized to dryness, and then dissolved with the Hypercarb column starting mobile phase (0.1% acetic acid). Next, the reconstituted void volume was injected on a Hypercarb column (150 mm × 4.6 mm, 5 μm) to quantify **Gh**, **(*R*)-d2Ih**, **(*S*)-d2Ih**,[42] **dGh**, **(*R*)-dSp**, **(*S*)-dSp**,[62] and **dZ**. Product peaks were quantified by their absorbance intensity at 240 nm followed by normalization of these intensities by each compound's extinction coefficient at 240 nm. The values for $\varepsilon_{240\ nm}$ (ddH_2O) are **dG** 14 080, **dOG** 14 300, **cyclo-dG** 14 080, **Gua** 14 080, **OG** 14 300,[15] **dSp** 3280,[22] **d2Ih** 2290,[8,35] **dGh** and **Gh** 2410,[54] and **dZ** 1780.[67] All values are in units of L mol^{-1} cm^{-1}.

■ ASSOCIATED CONTENT

Supporting Information

UPLC-ESI+-MS, HPLC-ESI+-MS, ESI+-MS/MS, reversed-phase HPLC, Hypercarb HPLC, UV−vis spectra, and product distribution tables. The Supporting Information is available free of charge on the ACS Publications website at DOI: 10.1021/acs.joc.5b00689.

■ AUTHOR INFORMATION

Corresponding Author

*E-mail: burrows@chem.utah.edu.

Notes

The authors declare no competing financial interest.

■ ACKNOWLEDGMENTS

The authors are grateful to Dr. James Muller (University of Utah) for his assistance with mass spectrometry and to the National Institutes of Health for financial support (R01 CA090689).

■ REFERENCES

(1) Sies, H. *Klin. Wochenschr.* **1991**, *69*, 965−968.
(2) Breen, A. P.; Murphy, J. A. *Free Radic. Biol. Med.* **1995**, *18*, 1033−1077.
(3) Ames, B. N.; Sheigenaga, M. K.; Hagen, T. M. *Biochem. Biophys. Acta* **1995**, *1271*, 165−170.
(4) Burrows, C. J.; Muller, J. G. *Chem. Rev.* **1998**, *98*, 1109−1152.
(5) Cadet, J.; Douki, T.; Gasparutto, D.; Ravanat, J.-L. *Mutat. Res.* **2003**, *531*, 5−23.
(6) Walling, C. *Acc. Chem. Res.* **1998**, *31*, 155−157.
(7) MacFaul, P. A.; Wayner, D. D. M.; Ingold, K. U. A. *Acc. Chem. Res.* **1998**, *31*, 159−162.
(8) Fleming, A. M.; Muller, J. G.; Ji, I.; Burrows, C. J. *Org. Biomol. Chem.* **2011**, *9*, 3338−3348.
(9) Cadet, J.; Douki, T.; Ravanat, J.-L. *Acc. Chem. Res.* **2008**, *41*, 1075−1083.
(10) Pratviel, G.; Meunier, B. *Chem.—Eur. J.* **2006**, *12*, 6018−6030.
(11) Gimisis, T.; Cismas, C. *Eur. J. Org. Chem.* **2006**, 1351−1378.
(12) Pogozelski, W. K.; Tullius, T. D. *Chem. Rev.* **1998**, *98*, 1089−1108.
(13) Steenken, S.; Jovanovic, S. V.; Bietti, M.; Bernhard, K. *J. Am. Chem. Soc.* **2000**, *122*, 2373−2374.
(14) Devasagayam, T. P.; Steenken, S.; Obendorf, M. S.; Schulz, W.; Sies, H. *Biochemistry* **1991**, *30*, 6283−6289.
(15) Henle, E. S.; Luo, Y.; Gassmann, W.; Linn, S. *J. Biol. Chem.* **1996**, *271*, 21177−21186.
(16) Grey, C. E.; Adlercreutz, P. *J. Agric. Food Chem.* **2006**, *54*, 2350−2358.
(17) Belmadoui, N.; Boussicault, F.; Guerra, M.; Ravanat, J.-L.; Chatgilialoglu, C.; Cadet, J. *Org. Biomol. Chem.* **2010**, *8*, 3211−3219.
(18) Pouget, J.-P.; Frelon, S.; Ravanat, J.-L.; Testard, I.; Odin, F.; Cadet, J. *Radiat. Res.* **2002**, *157*, 589−595.
(19) Dizdaroglu, M.; Rao, G.; Halliwell, B.; Gajewski, E. *Arch. Biochem. Biophys.* **1991**, *285*, 317−324.
(20) Douki, T.; Martini, R.; Ravanat, J.-L.; Turesky, R. J.; Cadet, J. *Carcinogenesis* **1997**, *18*, 2385−2391.
(21) Gedik, C. M.; Collins, A. *FASEB J.* **2005**, *19*, 82−84.
(22) Luo, W.; Muller, J. G.; Rachlin, E. M.; Burrows, C. J. *Org. Lett.* **2000**, *2*, 613−616.
(23) Slade, P. G.; Hailer, M. K.; Martin, B. D.; Sugden, K. D. *Chem. Res. Toxicol.* **2005**, *18*, 1140−1149.
(24) Misiaszek, R.; Crean, C.; Geacintov, N. E.; Shafirovich, V. *J. Am. Chem. Soc.* **2005**, *127*, 2191−2200.
(25) Niles, J. C.; Wishnok, J. S.; Tannenbaum, S. R. *Chem. Res. Toxicol.* **2004**, *17*, 1510−1519.
(26) Mangerich, A.; Knutson, C. G.; Parry, N. M.; Muthupalani, S.; Ye, W.; Prestwich, E.; Cui, L.; McFaline, J. L.; Mobley, M.; Ge, Z.; Taghizadeh, K.; Wishnok, J. S.; Wogan, G. N.; Fox, J. G.; Tannenbaum, S. R.; Dedon, P. C. *Proc. Natl. Acad. Sci. U.S.A.* **2012**, *109*, E1820−E1829.
(27) Hailer, M. K.; Slade, P. G.; Martin, B. D.; Sugden, K. D. *Chem. Res. Toxicol.* **2005**, *18*, 1378−1383.
(28) Henderson, P. T.; Delaney, J. C.; Muller, J. G.; Neeley, W. L.; Tannenbaum, S. R.; Burrows, C. J.; Essigmann, J. M. *Biochemistry* **2003**, *42*, 9257−9262.
(29) Delaney, J. C.; Neeley, W. L.; Delaney, J. C.; Essigmann, J. M. *Biochemistry* **2007**, *46*, 1448−1455.
(30) Cadet, J.; Berger, M.; Buchko, G. W.; Joshi, P. C.; Raoul, S.; Ravanat, J.-L. *J. Am. Chem. Soc.* **1994**, *116*, 7403−7404.
(31) Raoul, S.; Berger, M.; Buchko, G. W.; Joshi, P. C.; Morin, B.; Weinfeld, M.; Cadet, J. J. *Chem. Soc., Perkin Trans.* **1996**, *2*, 371−381.

DOI: 10.1021/acs.joc.5b00689
J. Org. Chem. 2015, 80, 6996−7007

(32) Gasparutto, D.; Ravanat, J.-L.; Gérot, O.; Cadet, J. *J. Am. Chem. Soc.* **1998**, *120*, 10283−10286.
(33) Kino, K.; Saito, I.; Sugiyama, H. *J. Am. Chem. Soc.* **1998**, *120*, 7373−7374.
(34) Kupan, A.; Saulière, A.; Broussy, S.; Seguy, C.; Pratviel, G.; Meunier, B. *Chem. Bio. Chem.* **2006**, *7*, 125−133.
(35) Ghude, P.; Schallenberger, M. A.; Fleming, A. M.; Muller, J. G.; Burrows, C. J. *Inorg. Chem. Acta* **2011**, *369*, 240−246.
(36) Vialas, C.; Claparols, C.; Pratviel, G.; Meunier, B. *J. Am. Chem. Soc.* **2000**, *122*, 2157−2167.
(37) Ye, W.; Sangaiah, R.; Degen, D. E.; Gold, A.; Jayaraj, K.; Koshlap, K. M.; Boysen, G.; Williams, J.; Tomer, K. B.; Mocanu, V.; Dicheva, N.; Parker, C. E.; Schaaper, R. M.; Ball, L. M. *J. Am. Chem. Soc.* **2009**, *131*, 6114−6123.
(38) Li, L.; Murthy, N. N.; Telser, J.; Zakharov, L. N.; Yap, G. P. A.; Rheingold, A. L.; Karlin, K. D.; Rokita, S. E. *Inorg. Chem.* **2006**, *45*, 7144−7159.
(39) Rokhlenko, Y.; Geacintov, N. E.; Shafirovich, V. *J. Am. Chem. Soc.* **2012**, *134*, 4955−4962.
(40) Banu, L.; Blagojevic, V.; Bohme, D. K. *J. Phys. Chem. B* **2012**, *116*, 11791−11797.
(41) Meister, A.; Anderson, M. E. *Annu. Rev. Biochem.* **1983**, *52*, 711−760.
(42) Fleming, A. M.; Alshykhly, O.; Orendt, A. M.; Burrows, C. J. *Tetrahedron Lett.* **2015**, *56*, 3191−3196.
(43) Fleming, A. M.; Muller, J. G.; Dlouhy, A. C.; Burrows, C. J. *J. Am. Chem. Soc.* **2012**, *134*, 15091−15102.
(44) Ye, Y.; Muller, J. G.; Luo, W.; Mayne, C. L.; Shallop, A. J.; Jones, R. A.; Burrows, C. J. *J. Am. Chem. Soc.* **2003**, *125*, 13926−13927.
(45) Extinction coefficients ($\varepsilon_{240\ nm}$) for **dSp** and **d2Ih** were assumed to be the same value; however, ring opening of the imidazole ring is anticipated to lead to a lower value of $\varepsilon_{240\ nm}$ for **d2Ih** compared to the ring closed **dSp** structure. Support for this claim was taken from the TDDFT calculations we have conducted to determine the UV spectroscopic properties of **d2Ih** and **dSp** (see refs 42 and 62). In these studies, UV−vis spectra were calculated with explicit and implicit solvation using the M06-2X functional and 6-311++G(2d,2p) basis set with implicit definition of water using the PCM, and these data allow a relative comparison of the $\varepsilon_{240\ nm}$ between **dSp** and **d2Ih** to be made. These calculations identify that **d2Ih** absorbs light at ∼70% of **dSp** (see Figure S23).
(46) Crespo-Hernandez, C. E.; Arce, R. *J. Photochem. Photobiol., B* **2004**, *73*, 167−175.
(47) Greenberg, M. M. *Acc. Chem. Res.* **2012**, *45*, 588−597.
(48) Frelon, S.; Douki, T.; Favier, A.; Cadet, J. *J. Chem. Soc., Perkin Trans. 1* **2002**, 2866−2870.
(49) Xiaoyun, X.; Muller, J. G.; Ye, Y.; Burrows, C. J. *J. Am. Chem. Soc.* **2008**, *130*, 703−709.
(50) Solivio, M. J.; Joy, T. J.; Sallans, L.; Merino, E. J. *J. Inorg. Biochem.* **2010**, *104*, 1000−1005.
(51) Lee, J.; Koo, N.; Min, D. B. *Comp. Rev. Food Sci. Food Safety* **2004**, *3*, 21−33.
(52) Yu, H.; Niles, J. C.; Wishnok, J. S.; Tannenbaum, S. R. *Org. Lett.* **2004**, *6*, 3417−3420.
(53) Steenken, S.; Jovanovic, S. V.; Bietti, M.; Bernhard, K. *J. Am. Chem. Soc.* **2000**, *122*, 2373−2374.
(54) Luo, W.; Muller, J. G.; Rachlin, E. M.; Burrows, C. J. *Chem. Res. Toxicol.* **2001**, *14*, 927−938.
(55) Fleming, A. M.; Burrows, C. J. *Chem. Res. Toxicol.* **2013**, *26*, 593−607.
(56) Hailer, M. K.; Slade, P. G.; Martin, B. D.; Sugden, K. D. *Chem. Res. Toxicol.* **2005**, *18*, 1378−1383.
(57) Lim, K. S.; Cui, L.; Taghizadeh, K.; Wishnok, J. S.; Chan, W.; DeMott, M. S.; Babu, I. R.; Tannenbaum, S. R.; Dedon, P. C. *J. Am. Chem. Soc.* **2012**, *134*, 18053−18064.
(58) Neeley, W. L.; Essigman, J. M. *Chem. Res. Toxicol.* **2006**, *19*, 491−505.
(59) Douki, T.; Spinelli, S.; Ravanat, J.-L.; Cadet, J. *J. Chem. Soc., Perkin Trans. 2* **1999**, 1875−1880.
(60) Cui, L.; Ye, W.; Prestwich, E. G.; Wishnok, J. S.; Taghizadeh, K.; Dedon, P. C.; Tannenbaum, S. R. *Chem. Res. Toxicol.* **2013**, *26*, 195−202.
(61) Tomaszewska, A.; Mourgues, S.; Guga, P.; Nawrot, B.; Pratviel, G. *Chem. Res. Toxicol.* **2012**, *25*, 2505−2512.
(62) Fleming, A. M.; Orendt, A. M.; He, Y.; Zhu, J.; Dukor, R. K.; Burrows, C. J. *J. Am. Chem. Soc.* **2013**, *135*, 18191−18204.
(63) Ye, W.; Sangaiah, R.; Degen, D. E.; Gold, A.; Jayaraj, K.; Koshlap, K. M.; Boysen, G.; Williams, J.; Tomer, K. B.; Ball, L. M. *Chem. Res. Toxicol.* **2006**, *19*, 506−510.
(64) Li, L.; Karlin, K. D.; Rokita, S. E. *J. Am. Chem. Soc.* **2005**, *127*, 520−521.
(65) Fleming, A. M.; Alshykhly, O.; Zhu, J.; Muller, J. G.; Burrows, C. J. *Chem. Res. Toxicol.* **2015**, *28*, 1292−1300.
(66) Kanvah, S.; Joseph, J.; Schuster, G. B.; Barnett, R. N.; Cleveland, C. L.; Landman, U. *Acc. Chem. Res.* **2010**, *43*, 280−287.
(67) Matter, B.; Malejka-Giganti, D.; Csallany, A. S.; Tretyakova, N. *Nucleic Acids Res.* **2006**, *34*, 5449−5460.
(68) Huang, H.; Das, R. S.; Basu, A. K.; Stone, M. P. *J. Am. Chem. Soc.* **2011**, *133*, 20357−20368.
(69) Eckenroth, B. E.; Fleming, A. M.; Sweasy, J. B.; Burrows, C. J.; Doublié, S. *Biochemistry* **2014**, *53*, 2075−2077.
(70) Karwowski, B.; Dupeyrat, F.; Bardet, M.; Ravanat, J.-L.; Krajewski, P.; Cadet, J. *Chem. Res. Toxicol.* **2006**, *19*, 1357−1365.

DOI: 10.1021/acs.joc.5b00689
J. Org. Chem. 2015, 80, 6996−7007